

# Matrix-assisted ultraviolet laser-desorption ionization time-of-flight mass spectrometry of sulfated mannans from the red seaweed *Nothogenia fastigiata*

Rosa Erra-Balsells<sup>a</sup>, Adriana A. Kolender<sup>a</sup>, María C. Matulewicz<sup>a</sup>, Hiroshi Nonami<sup>b</sup>,  
Alberto S. Cerezo<sup>a,\*</sup>

<sup>a</sup> Departamento de Química Orgánica, Facultad de Ciencias Exactas y Naturales, Universidad de Buenos Aires, Pabellón 2, Ciudad Universitaria, 1428 Buenos Aires, Argentina

<sup>b</sup> Plant Biophysics/Biochemistry Research Laboratory, College of Agriculture, Ehime University, 3-5-7 Tarumi, Matsuyama 790-8566, Japan

Received 29 October 1999; accepted 25 May 2000

## Abstract

Matrix-assisted ultraviolet laser-desorption ionization time-of-flight mass spectrometry (UV-MALDI-TOF-MS) was applied to sulfated *xylo*-mannan fractions from *Nothogenia fastigiata* in order to determine their molecular weights and distribution profiles. The number-average molecular weight calculated from the spectra was similar to that determined by chemical end-group analysis for the lower molecular weight fractions. For the other fractions, the number-average molecular weight was lower than that chemically determined; the increased difference may be attributed to higher desorption difficulties and, consequently, mass-dependent discrimination. A reconstructed spectrum, using the peaks obtained from all the fractions, suggested an unimodal distribution. The best results were obtained by using 2,5-dihydroxybenzoic acid as matrix doped with 1-hydroxyisoquinoline and with harmane and *nor*-harmane. © 2000 Elsevier Science Ltd. All rights reserved.

**Keywords:** Sulfated polysaccharides; Sulfated *xylo*-mannans; UV-MALDI-TOF-MS

## 1. Introduction

The red seaweed *Nothogenia fastigiata* synthesizes a complex system of polysaccharides comprising neutral xylans of the  $\beta$ -D-(1  $\rightarrow$  3)-,  $\beta$ -D-(1  $\rightarrow$  4)-‘mixed linkage’ type [1–3] and sulfated polysaccharides. These sulfated polysaccharides are a family of  $\alpha$ -(1  $\rightarrow$  3)-linked D-mannans 2- and 6-sulfated and having single stubs of  $\beta$ -(1  $\rightarrow$  2)-linked D-xylose [4–6]

(Fig. 1), and sulfated xylogalactans [7,8] with a backbone formed by alternating 3-linked  $\beta$ -D-galactopyranose and 4-linked  $\alpha$ -L-galactopyranose. The 4-linked residues are either 6-sulfated having single stubs of (1  $\rightarrow$  3)-linked D-xylose or (1  $\rightarrow$  3)-linked galactose, 3-sulfated or non-substituted. The  $\beta$ -D-galactopyranosyl units are non-substituted or 4-sulfated. The whole system of polysaccharides showed erratic solubility behavior associated with composition-, temperature-, time- and conformation-dependent molecular associations [4–8]. These structures have been studied by chemical and spectroscopic methods [4–6,8].

\* Corresponding author. Tel./fax: + 54-11-45763346.  
E-mail address: cerezo@qo.fcen.uba.ar (A.S. Cerezo).

Matrix-assisted ultraviolet laser-desorption ionization time-of-flight mass spectrometry (UV-MALDI-TOF-MS) is a valuable technique for the determination of molecular weights of proteins [9–11]. Nevertheless when used with polysaccharides good results were only obtained for samples with molecular weights lower than 6000. This limitation is probably related, at least in part, to the structural complexity [12] and to molecular interactions often found in these biopolymers. Recent studies with low-molecular-weight laminarans [13], fructans [14], dextrans and maltodextrins [15] illustrated the power of positive-ion mode MALDI-MS for defining the degree of polymerization profiles of polysaccharides. In this mode, sialic acid containing oligosaccharides generally produced the sodium adduct of the sodium salt giving much weaker signals than the neutral sugars [16]. Very few MALDI-MS analyses of sulfated oligosaccharides [17–19] have been reported, and in all of them samples with molecular weights below 2000 were analyzed. These oligosaccharides were detected in the negative-ion mode [17–19], and it was suggested that the presence of sulfate groups in the structure stabilized the corresponding anionic form [18].

The 2,5-dihydroxybenzoic acid (gentisic acid, DHB) proved to be the most appropriate matrix for examination of neutral or sialic acid-containing oligosaccharide mixtures [16] as well as neutral polysaccharides [13–15] in the positive-ion mode. This matrix has been also shown to be suitable for the quantification of oligosaccharides and to produce a signal that reflects sample concentrations over several orders of magnitude [20]. When the low-molecular-weight sulfated oligosaccharides were analyzed, the 9*H*-pyrido[3,4-*b*]indoles ( $\beta$ -carboline) were shown to be useful as UV-MALDI matrices [18].

In order to achieve this goal with sulfated polysaccharides, in the present project we designed several experiments employing different MALDI matrices [3,5-dimethoxy-4-hydroxycinnamic acid (sinapinic acid, SA),  $\alpha$ -cyano-4-hydroxycinnamic acid (CHC), DHB,  $\beta$ -carboline (*nor*-harmane, harmane and harmine)] and doped matrices [DHB–1-hydroxyisoquinoline (DHB–HIC) and DHB– $\beta$ -carboline], and three different methods for sample preparation. All spectra were obtained in positive and linear modes as the average of 50 laser shots. Besides, inspection of all the

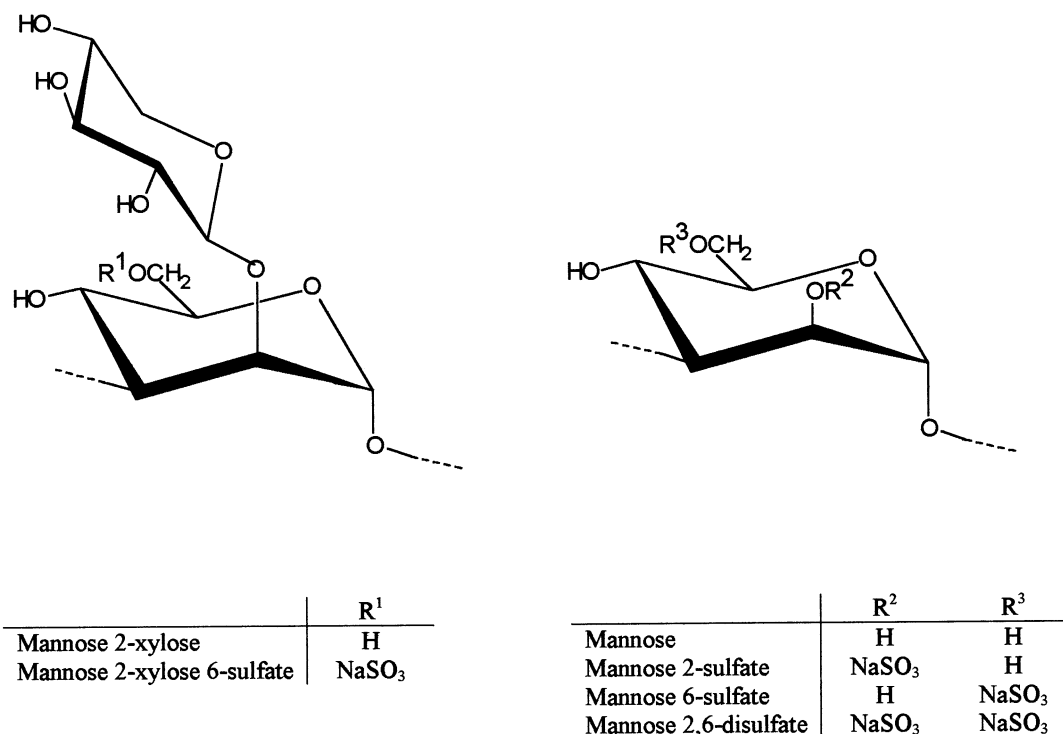


Fig. 1. Substitution pattern for the xylo-mannans from *N. fastigiata*.

Table 1

Composition and chemically determined degree of polymerization (dp) of the sulfated *xylo*-mannan fractions

Fraction	Sugar composition <sup>a</sup> (mol%)		Sulfate (% NaSO <sub>3</sub> )	Counterion (% equiv)			Weight of the average unit <sup>b</sup>	Average dp <sup>c</sup>
	Man	Xyl		Ca <sup>2+</sup>	Mg <sup>2+</sup>	Na <sup>+</sup>		
2'	62.3	21.5	17.6	73.8	17.2	9.0	271	44
3	73.8	20.4	26.1	48.1	20.8	31.0	288	136
4'	81.6	16.4	26.0	72.5	22.1	5.4	264	83
5'	97.5	2.5	15.3	49.7	15.0	53.3	197	32
6'	97.9	2.1	31.7	77.1	17.6	5.2	249	120

<sup>a</sup> Contamination with galactose from the sulfated galactan to 100.0%.<sup>b</sup> From molar ratios xylose:sulfate:mannose of Ref. [6].<sup>c</sup> Calculated using the molecular weights of Ref. [6].

solid samples ready to be analyzed by UV-MALDI was performed in order to see the influence of the sulfated polysaccharides under study on the crystallization of the matrix.

As result of our studies, we herein report the successful application of UV-MALDI-TOF-MS for the analysis of the family of sulfated *xylo*-mannans from the red seaweed *N. fastigiata*, with molecular weights in the range 2000–45,000 and with strong molecular interactions.

## 2. Results

The sulfated polysaccharides from *N. fastigiata* were precipitated with Cetrimide, and the insoluble complexes were subjected to fractional solubilization in solutions of increasing sodium chloride concentration (0.5–4.0 M); in this way, five *xylo*-mannan fractions were separated and further purified by redissolution in sodium chloride solutions of the corresponding concentration. Table 1 shows their composition and the chemically determined degree of polymerization. Considering the fractionation procedure, the presence of high percentages of Ca<sup>2+</sup> and Mg<sup>2+</sup> (determined by flame atomic absorption spectrometry) that neutralized most of the sulfate groups was completely unexpected.

Among all the matrices tested, only the mixtures of DHB–HIC and DHB–*nor*-har-

mane (*nor*-harmane: 9*H*-pyrido[3,4-*b*]indole) DHB–harmane (harmane: 1-methyl-9*H*-pyrido[3,4-*b*]indole) worked as proper MALDI matrices. These mannans were detected only in the positive-ion mode, and only the mentioned doped matrices provided good spectra in terms of signal strength and background level.

Table 2 indicates the  $m/z$ , the normalized intensities (heights,  $I_n$ ) of all the peaks observed for the fractions in the different recorded spectra, using DHB–HIC as matrix, and the corresponding corrected values ( $I_c$ ), taking into account the percentage contribution of each fraction to the 'whole' sample.  $I_n$  and  $I_c$  were calculated according to the following equations:

$$I_n = I_p/I_t$$

where  $I_n$  is the normalized peak intensity,  $I_p$  is the peak intensity (mV) and  $I_t$  is the total intensity (mV) of the spectrum and

$$I_c = I_n X$$

where  $I_c$  is the corrected peak intensity and  $X$  is the percentage contribution of the fraction to the whole polysaccharide sample [6].

Each spectrum does not give an unimodal distribution of molecular weights, as expected for plant polysaccharides, possibly due to the very small amount of signals. These peaks usually show a maximum followed by satellite signals of lower intensity that suggest an

asymmetric envelope. Although the peaks are obtained at random, always the same group of signals is observed for each fraction; this pattern is consistent with signals not reflecting sample concentrations due to erratic desorption–ionization processes. Fig. 2 shows two typical spectra of Fraction 4' carried out under identical experimental conditions. Table 3 gives the number-average molecular weights ( $M_n$ ) of the *xylo*-mannan fractions, calculated using the  $m/z$  values and normalized peak intensities of Table 2 according to:

$$M_n = \Sigma I_{ni} M_i / \Sigma I_{ni}$$

( $I_{ni}$  is the normalized intensity of the peak  $i$  and  $M_i$  is the  $m/z$  value of the peak  $i$ ), and the corresponding number-average molecular weights determined by end-group analysis;

similar values were observed for Fractions 2' and 5' by the two methods.

Fig. 3 shows a reconstructed spectrum of Fraction 2' using the normalized intensities of the 23  $m/z$  peaks from all the spectra recorded for this fraction indicated in Table 2. This reconstructed spectrum suggests an unimodal distribution function consistent with signals not reflecting the sample concentration and with the fact that the sample is only a small part of the original *xylo*-mannan family. No reconstructions were carried out for the other fractions because not enough peaks were obtained in the corresponding spectra.

Considering that the fractions were obtained through a fractionation procedure with arbitrary boundaries, they can not be considered as 'different' sulfated *xylo*-mannans but as parts of the family of these polysaccharides. On this basis, a reconstructed spectrum of this

Table 2

Normalized intensities and corrected values of the  $m/z$  peaks of the sulfated *xylo*-mannan fractions <sup>a</sup>

Peak	$m/z$	Fraction	$I_n$	$I_c$	Peak	$m/z$	Fraction	$I_n$	$I_c$
1	45,270	3	0.0229	0.776	30	12,275	2'	0.0587	0.740
2	45,000	3	0.0200	0.678	31	12,137	2'	0.0784	0.988
3	44,930	3	0.0221	0.749	32	11,633	2'	0.0312	0.393
4	44,200	3	0.0024	0.081	33	11,568	2'	0.0263	0.331
5	42,000	3	0.0057	0.193	34	11,082	2'	0.0133	0.168
6	41,701	3	0.0167	0.566	35	10,373	6'	0.0376	0.699
7	40,400	3	0.0048	0.163	36	9997	3	0.0130	0.441
8	33,607	6'	0.0345	0.642	37	9989	4'	0.0870	1.418
9	31,270	3	0.0048	0.163	38	9405	2'	0.0189	0.238
10	30,790	3	0.0164	0.556	39	9302	2'	0.0526	0.663
11	30,750	3	0.0714	2.420	40	9250	2'	0.0072	0.907
12	29,000	6'	0.0179	0.333	41	8491	2'	0.0667	0.844
13	25,400	3	0.0067	0.227	42	8091	2'	0.0051	0.064
14	22,270	3	0.0023	0.078	43	6602	5'	0.0185	0.344
15	20,797	3	0.0188	0.637	44	6190	2'	0.0127	0.160
16	20,323	4'	0.0185	0.302	45	6016	5'	0.0161	0.299
17	20,300	6'	0.0179	0.333	46	5982	5'	0.0179	0.333
18	19,720	4'	0.0851	1.387	47	5710	5'	0.0179	0.333
19	19,300	2'	0.0048	0.060	48	5600	5'	0.0145	0.270
20	19,237	3	0.0196	0.664	49	5500	2'	0.0313	0.394
21	17,500	2'	0.0080	0.101	50	5260	3	0.0087	0.295
22	17,000	3	0.0164	0.556	51	5238	2'	0.0652	0.821
23	16,245	2'	0.0555	0.699	52	4850	5'	0.0145	0.270
24	14,330	6'	0.0392	0.729	53	4000	2'	0.0070	0.088
25	13,673	2'	0.0070	0.088	54	3533	2'	0.0141	0.178
26	13,600	3	0.0103	0.349	55	3300	2'	0.0101	0.127
27	13,326	3	0.0156	0.529	56	2556	6'	0.0329	0.611
28	13,180	3	0.0049	0.166	57	2439	2'	0.0175	0.221
29	12,439	2'	0.0266	0.335	58	2113	2'	0.0093	0.116

<sup>a</sup> See text.

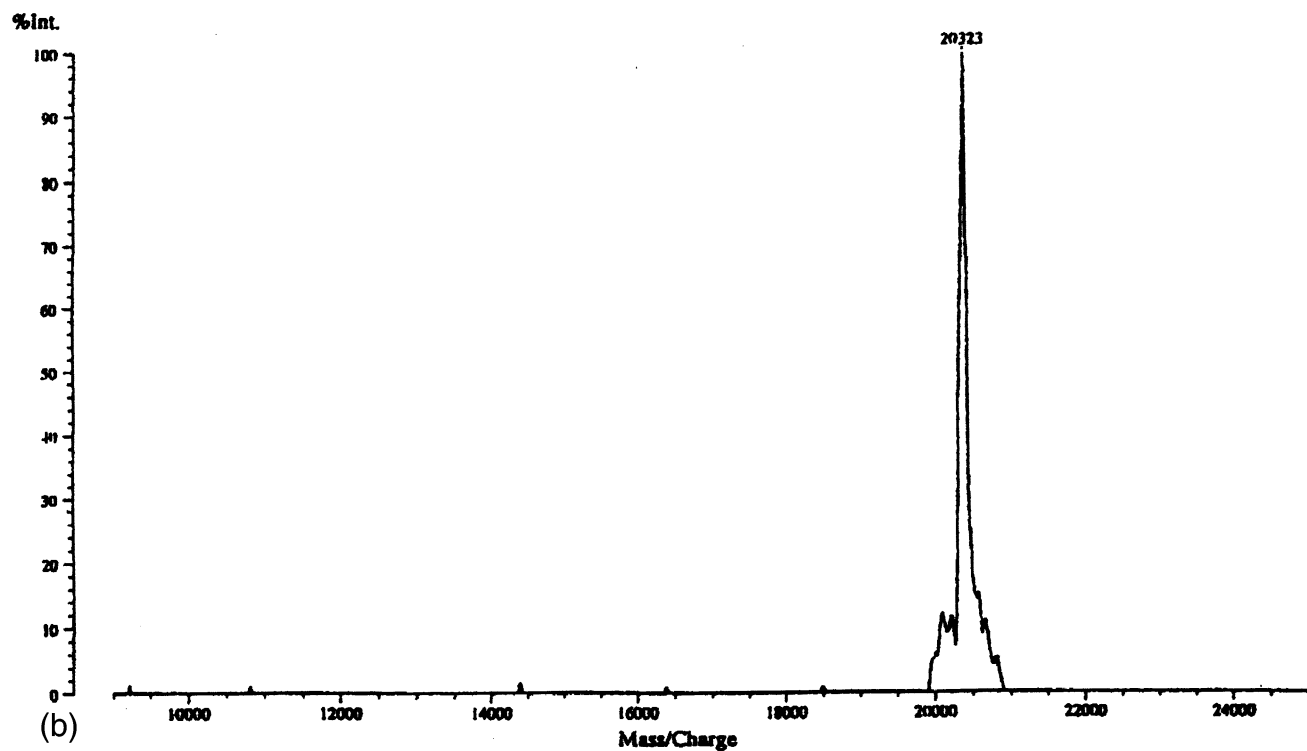
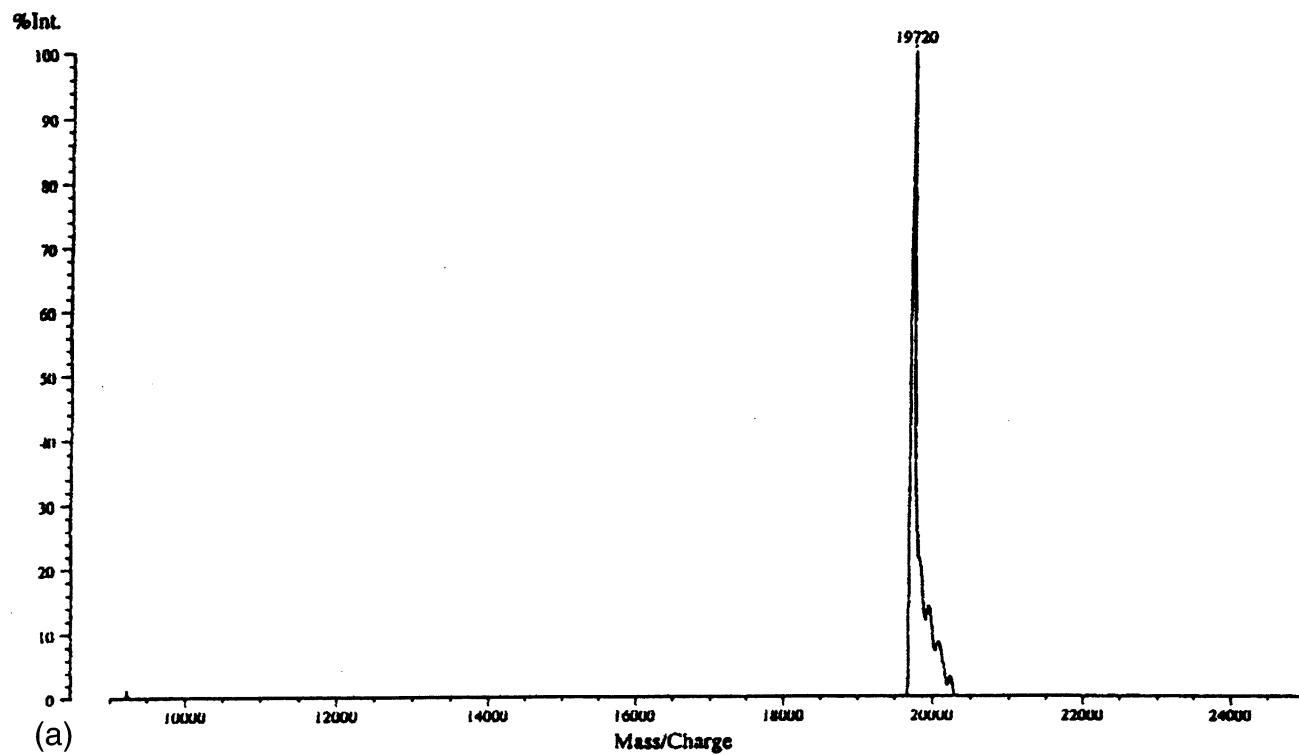


Fig. 2. Typical UV-MALDI-TOF mass spectra obtained from Fraction 4' (matrix: DHB-HIC,  $\lambda$ : 337 nm; see Section 4) consistent with erratic desorption-ionization of the sample.

Table 3  
Number-average molecular weights from MALDI and end-group analysis of the sulfated *xylo*-mannan fractions

Fraction	$M_n^a$	$M_n^b$
2'	9808	12,000
3	29,234	39,100
4'	15,337	21,900
5'	5833	6400
6'	17,099	30,000

<sup>a</sup> Number-average molecular weight calculated using the  $m/z$  values and the corresponding normalized peak intensities.

<sup>b</sup> Number-average molecular weight determined by end-group analysis.

family was obtained using the normalized intensities of the 58  $m/z$  peaks from all the spectra and taking into account the percentage contribution of each fraction to the 'whole' sample (Table 2, Fig. 4). This reconstructed spectrum suggests again a statistical distribution profile.

Cesium chloride has been recommended as useful to increase the cationizing process in carbohydrates [21]. It is interesting to point out that in the present study no important effect was observed by addition of this doping salt to the samples.

Finally, as it is shown in Figs. 5–8 and described in detail in Section 4, the crystalliza-

tion of DHB was clearly improved not only by adding the doping co-matrix (HIC, *nor*-harmane or harmane) but also by adding the *xylo*-mannan.

### 3. Discussion

These sulfated polysaccharides are a family of  $\alpha$ -(1  $\rightarrow$  3)-linked D-mannans 2- and 6-sulfated and having single stubs of  $\beta$ -(1  $\rightarrow$  2)-linked D-xylose [4–6]. These products showed erratic solubility behavior associated with composition-, temperature-, time- and conformation-dependent molecular associations [4–8]. The composition of the fractions (Table 1) indicates that the fractionation of the sulfated *xylo*-mannan system depends mainly on the amount of single stubs of D-xylose and that only fractions with similar quantities of side-chains were separated according to the percentage of sulfate [6]. This suggests that the major factor of insolubilization was the formation of packed aggregates of macromolecules, since this process was facilitated by the formation of the insoluble Cetrimide salts. The *xylo*-mannans still contained divalent counterions after precipitation with Cetrimide, followed by redissolution of the insoluble complexes and further purification of the frac-

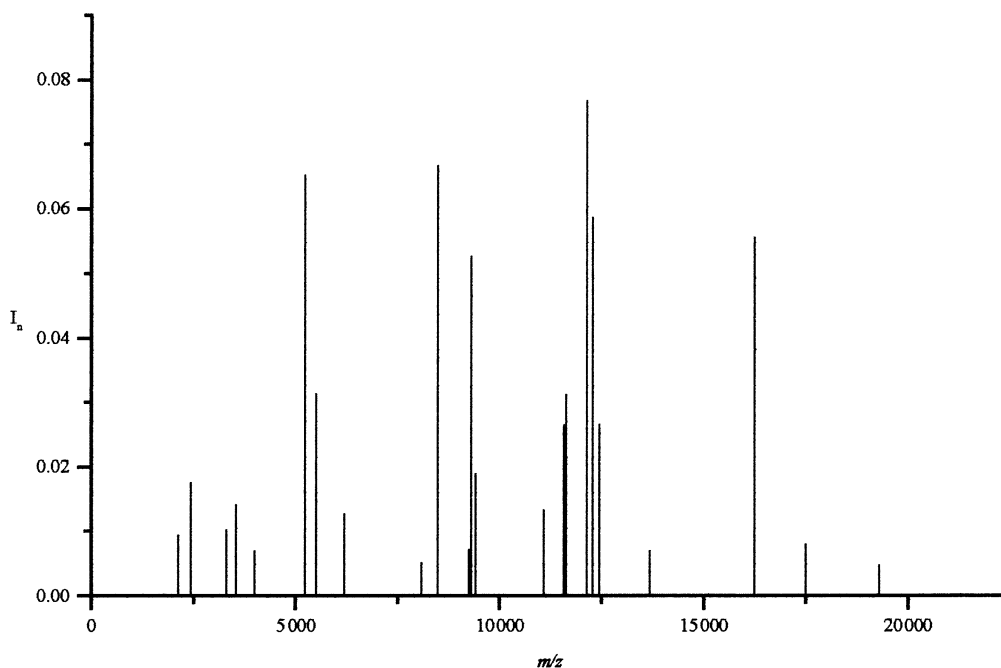


Fig. 3. Reconstructed spectrum of Fraction 2' using the normalized intensities ( $I_n$ ) of the 23  $m/z$  peaks indicated in Table 2.

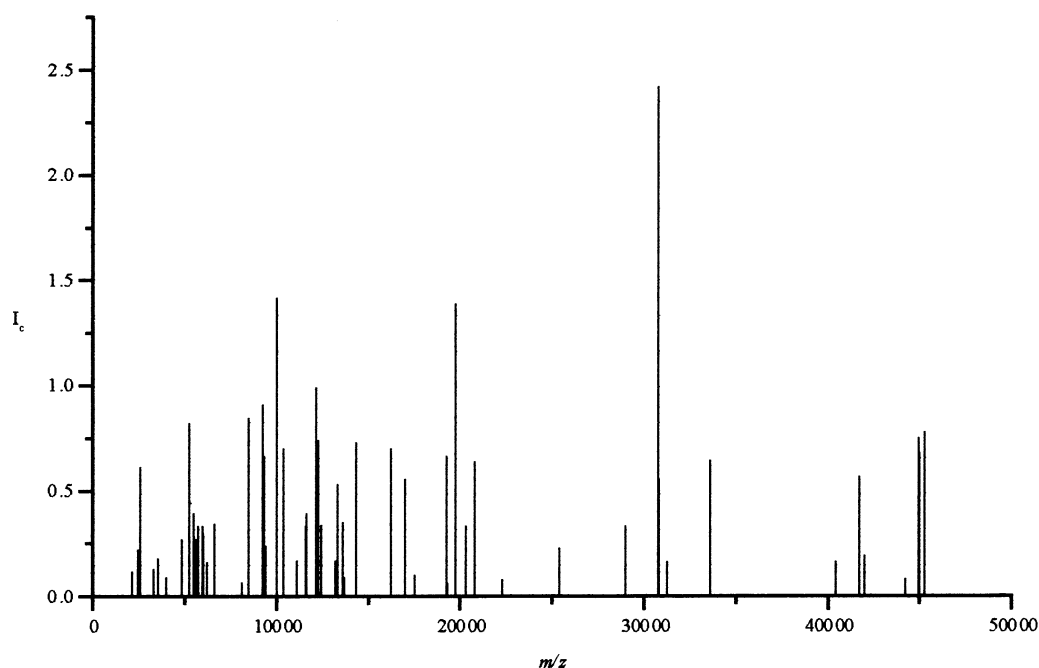


Fig. 4. Reconstructed spectrum of the 'whole' sample using the normalized and corrected intensities ( $I_c$ ) of Table 2.

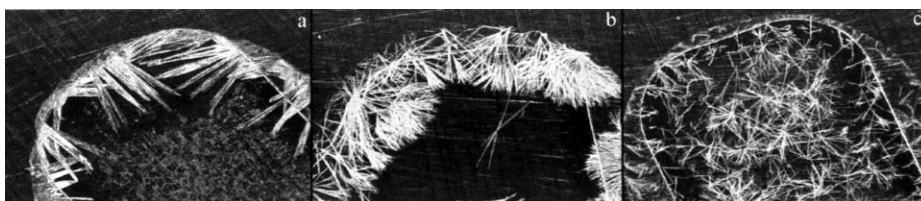


Fig. 5. Images of the matrices: (a) DHB, (b) and (c) harmane. Magnification  $150\times$ .

tions at high sodium chloride concentrations. This result suggests that these divalent ions are not present as simple counterions, but that they are tightly complexed with the polysaccharides, in agreement with the strong tendency shown by these products to form soluble and insoluble aggregates [8]. In fact, Fraction 2' was isolated as a complex of a *xylo*-mannan with small amounts of a xylan and galactan [8]; the rest of the fractions contained no xylan and small-to-negligible amounts of galactan.

It was known that one of the strongest attributes of MALDI is the ability to analyze proteins [9–12], and it was thought that this ability could be applied to the study of the molecular weight dispersions of the sulfated *xylo*-mannan fractions, in spite of their structural complexity, their ability to form unspecific aggregates, and the fact that these samples only partially represent, after frac-

tionation and purification, the original biosynthesized product.

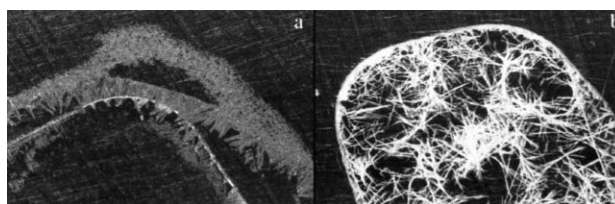


Fig. 6. Images of selected analyte-matrix systems: (a) Fraction 4'-DHB and (b) Fraction 4'-harmane. Magnification  $150\times$ .

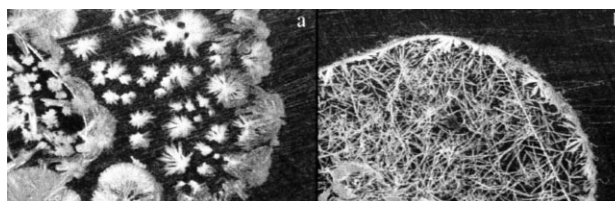


Fig. 7. Images of the doped matrices: (a) DHB-HIC and (b) DHB-harmane. Magnification  $150\times$ .

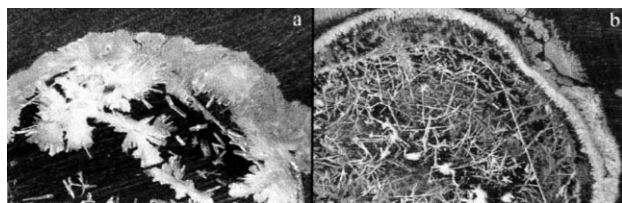


Fig. 8. Images of selected analyte-doped matrix systems: (a) Fraction 4'-DHB-HIC and (b) Fraction 4'-DHB-harmane. Magnification  $150\times$ .

It is important to point out several facts in the spectra of the sulfated *xylo*-mannans: (a) They show a broad range of  $m/z$  values (2113–45,270 amu). To the best of our knowledge, this is the first report on MALDI spectra of high molecular weight polysaccharides. (b) They do not show the unimodal distributions expected for molecular weight dispersions of plant polysaccharides [13–15]. (c) They consist of only a few peaks and in some cases of a single one; besides, these appear at random suggesting low yield erratic desorption–ionization processes [20].

In the case of the lower molecular weight Fractions 2' and 5', the calculated and the chemically determined molecular weights are similar suggesting that most of the ions are molecular ions. In Fractions 3, 4' and 6' the number-average molecular weights calculated from the spectra are lower than those determined by the end-group procedure. It is noteworthy that the difference between the calculated and the chemically determined molecular weights (Tables 1 and 3) increases with the molecular weight, suggesting higher desorption difficulties and consequently mass-dependent discrimination [20]. It is known that in MALDI-MS deviation between apparent and real size distribution is due mainly to a preferential desorption and ionization of smaller analyte molecules that suppress desorption and ionization of larger molecules [20]. The fact that the chemically determined molecular weight is invariably higher than that calculated from the MALDI spectra suggests that monocharged cluster ions are not present, but it is not possible to discard the presence of poly-charged ions.

Thus, when an addition spectrum was obtained for Fraction 2', using the 23  $m/z$  peaks derived from several spectra, an unimodal dis-

tribution was suggested, disregarding the uneven low intensity of the peaks. Considering that the fractions are arbitrary and that they do not represent 'different' polysaccharides, but only parts of the family of sulfated *xylo*-mannans biosynthesized by the seaweed, a reconstructed spectrum of the 'whole' sample was determined using the peaks from all the spectra of the five fractions (Fig. 4). The spectrum suggests an unimodal distribution in spite of that the peaks do not represent the concentrations in the sample. Maltodextrin and dextran samples with molecular weights in the range of low masses (less than 6000) showed no mass-dependent discrimination [15], but the whole-sample reconstructed spectrum of the *xylo*-mannans suggests that this could happen in samples with strong association behavior and higher molecular weights. This association behavior could depend not only on the structural features of the sulfated *xylo*-mannans but also on the formation of non-stoichiometric calcium-dependent complexes.

#### 4. Experimental

**General.**—Isolation and fractionation of the sulfated polysaccharides of *N. fastigiata*, has been carried out as previously described [4–6], and led to Fractions 2–6. Fractions 2, 4, 5, and 6 were further purified yielding Fractions 2', 4', 5', and 6' [5,6]. Molecular weights were determined by the colorimetric method of Park and Johnson [22].  $\text{Na}^+$ ,  $\text{Ca}^{2+}$  and  $\text{Mg}^{2+}$  determinations were carried out by flame atomic absorption spectrometry using a Shimadzu AA 6800 atomic absorption spectrometer.

**Matrix-assisted ultraviolet laser-desorption time-of-flight mass spectrometry**

**Matrix chemicals.**  $\beta$ -Carbolines (*nor*-harmane: 9*H* - pyrido[3,4 - *b*]indole; harmane: 1-methyl - 9*H* - pyrido[3,4 - *b*]indole; harmine: 1-methyl-7-methoxy-9*H*-pyrido[3,4-*b*]indole), 2,5-dihydroxybenzoic acid (gentisic acid, DHB), 3,5-dimethoxy-4-hydroxycinnamic acid (sinapinic acid, SA),  $\alpha$ -cyano-4-hydroxycinnamic acid (CHC) and 1-hydroxyisoquinoline (HIC) were purchased from Aldrich Chemical Co.



**Calibrant chemicals.** Proteins, i.e., bovine insulin (I5500, MW 5733.5), aprotinin (A1153, MW 6512), ribonuclease A (R5500, MW 13,700), lysozyme (L6876, MW 14,307), myoglobin (M0630, MW 16,950), trypsin (T8003, MW 23,290) and protease (Subtilisin Carlberg P5380, MW 27,288.4) were obtained from Sigma Chemical Co.

**Probe support materials.** The stainless steel 20 sample slides were purchased from Shimadzu Co., Japan.

**Organic solvents.** MeCN and EtOH (Sigma–Aldrich HPLC grade), TFA (Merck) were used as purchased without further purification. Water of very low conductivity (Milli Q grade; 56–59 nS/cm with PURIC-S, ORUGANO Co., Ltd., Tokyo, Japan) was used.

**Instruments.** Measurements were performed using the UV laser desorption time-of-flight mass spectrometer Shimadzu Kratos, Compact MALDI III (Shimadzu, Kyoto, Japan), equipped with a pulsed nitrogen laser ( $\lambda = 337$  nm; pulse width = 3 ns). The analyzer was used at an accelerating voltage of 20 kV for measuring high-mass samples. Ions were obtained by irradiation of the sample just above the threshold laser power. Thus, the irradiance used for producing a mass spectrum was analyte dependent. Usually 50 spectra were accumulated as maximum. All samples were measured in the linear and reflectron modes, and as routine in both the positive- and the negative-ion modes, although no signals were detected in the latter mode.

**Sample preparation.** Matrix stock solutions were made by dissolving 20 mg of the selected compound (*nor*-harmane, harmane, DHB) in 1 mL of MeCN–0.1% TFA (2:3, v/v). As has been previously described [21,23], in order to use HIC as additive for DHB, 0.2 M DHB and 0.06 M HIC in 1:1 water–MeCN were prepared; in sample preparation Methods A and B (see later), the so called matrix solution was prepared as a 3:1 mixture of the former and the latter solutions. The same protocol was followed when  $\beta$ -carboline (*nor*-harmane or harmane) were used, instead of HIC, as the additive for DHB. Analyte solutions of 0.10 mg/mL were freshly prepared by dissolving the polysaccharides in pure water. For calibra-

tion purposes, protein solutions of 10 pmol/ $\mu$ L were freshly prepared by dissolving each protein in 0.1% TFA.

In the present work, three sample preparation methods slightly different from those previously described [18,23] have been used. In the first method (Method A), prior to the sample preparation, 1.0  $\mu$ L of the matrix solution was placed on each sample probe plate ( $2 \times 1.5$  mm) in order to wash it, and then it was sucked dry with the same pipette tip. In order to make the analyte–matrix deposit, typically 0.5  $\mu$ L of the analyte solution was placed on the sample probe plate with the same pipette tip that was used for washing, followed by addition of 1.0  $\mu$ L of the matrix solution covering the analyte solution, and then the solvent was removed by blowing air at rt. Thus, 1.5  $\mu$ L as total volume of both solutions was used. In the second procedure (Method B), 0.5  $\mu$ L of the matrix solution were placed on the sample probe plate, and the solvent was removed by blowing air. Subsequently, 0.5  $\mu$ L of the analyte solution was added to cover the matrix, and the solvent was removed by blowing air. Then, two additional portions (0.5  $\mu$ L) of the matrix solution were deposited on the same sample probe plate. Thus, the matrix to analyte ratio used was 3:1 (v/v) and the matrix and analyte solution loading sequence was: (i) matrix (0.5  $\mu$ L), (ii) analyte (0.5  $\mu$ L), (iii) matrix (0.5  $\mu$ L), (iv) matrix (0.5  $\mu$ L). In Method C, the application of DHB–HIC as a matrix for polysaccharides (analyte) showed the best results when the matrix and analyte solutions were deposited and dried by blowing air according to the following sequence: (i) DHB (0.5  $\mu$ L), (ii) DHB (0.5  $\mu$ L), (iii) HIC (0.5  $\mu$ L), (iv) DHB (0.5  $\mu$ L), (v) analyte (0.5  $\mu$ L). This DHB–HIC ratio (3:1, v/v) is different from that previously reported by Mohr et al. [21] as optimum in their experimental conditions. The DHB– $\beta$ -carboline (*nor*-harmane or harmane) doped matrix was used following the same protocol.

**Salt doping of the samples with CsCl.** The second and the third protocols above described (Methods B and C) were followed when  $\beta$ -carboline, DHB, DHB–HIC and DHB– $\beta$ -carboline were used as matrix, and

CsCl was added as the doping agent. When 0.5  $\mu\text{L}$  of an aqueous CsCl solution (0.25 M) was added to the sample, the sequence used to load the solutions on the sample probe plate was: Method B (i) matrix (0.5  $\mu\text{L}$ ), (ii) analyte (0.5  $\mu\text{L}$ ), (iii) CsCl (0.5  $\mu\text{L}$ ), (iv) matrix (0.5  $\mu\text{L}$ ), (v) matrix (0.5  $\mu\text{L}$ ); Method C (i) DHB (0.5  $\mu\text{L}$ ), (ii) DHB (0.5  $\mu\text{L}$ ), (iii) HIC (0.5  $\mu\text{L}$ ), (iv) DHB (0.5  $\mu\text{L}$ ), (v) analyte (0.5  $\mu\text{L}$ ), (vi) CsCl (0.5  $\mu\text{L}$ ).

Inspection of crystals from solids ready to be used as samples was carried out with a Stereoscopic microscope (NIKON Optiphot, Tokyo, Japan) with magnification  $400\times$  and digital images were obtained with a high-resolution digital microscope (Keyence VH-6300, Keyence Corporation, Osaka, Japan) with magnification  $150\times$ . The recorded images (Figs. 5–8) showed that, in our hands: (a) DHB alone exhibited preferential crystallization from the edge of the deposit and large white crystals were observed (Fig. 5(a)); (b) harmane alone showed crystals in the edge or small crystals distributed on the solid deposit (Fig. 5(b,c)); (c) DHB showed preferential crystallization from the edge of the polysaccharide deposit and small white crystals were observed (Fig. 6(a)); (d) harmane showed after loading the matrix on the sample deposit, a white emulsion that then became transparent and yielded rather uniform crystals distributed in a non homogeneous way on the sample surface (Fig. 6(b)); (e) doped DHB matrices (DHB–HIC and DHB–harmane, Fig. 7) showed a lower amount of crystals distributed on the sample surface than the system constituted by the doped DHB matrix and the polysaccharide (DHB–HIC–polysaccharide and DHB–harmane–polysaccharide, Fig. 8). The images shown in Fig. 6 correspond to samples prepared according to Method B, and those in Figs. 7 and 8 are images of samples prepared according to Method C.

**Spectrum calibration.** Spectra were calibrated by use of  $\text{Na}^+$  and standard chemicals such as bovine insulin, aprotinin, ribonuclease A, lysozyme, myoglobin, trypsin and protease (external calibrant reagents) and  $\beta$ -carboline (internal calibrant reagents). The Kratos Kompact calibration program was used.

## Acknowledgements

The authors are indebted to the National Research Council of Argentina (CONICET) and the University of Buenos Aires (UBA) for financial support. A.S.C., R.E.-B. and M.C.M. are Research Members of CONICET. UV-MALDI-TOF-MS experiments were performed as part of the Academic Agreement between R.E.-B. (FCEyN-UBA, Argentina) and H.N. (CA-EU, Japan) with the facilities of the High Resolution Liquid Chromatography-Integrated Mass Spectrometer System of the United Graduated School of Agricultural Sciences (Ehime University, Japan).

## References

- [1] A.S. Cerezo, A. Lezerovich, R. Labriola, D.A. Rees, *Carbohydr. Res.*, 19 (1971) 289–296.
- [2] A.S. Cerezo, *Carbohydr. Res.*, 22 (1972) 209–211.
- [3] M.C. Matulewicz, A.S. Cerezo, R.J. Jarret, N. Syn, *Int. J. Biol. Macromol.*, 14 (1992) 29–32.
- [4] M.C. Matulewicz, A.S. Cerezo, *Carbohydr. Polym.*, 7 (1987) 121–132.
- [5] A.A. Kolender, M.C. Matulewicz, A.S. Cerezo, *Carbohydr. Res.*, 273 (1995) 179–185.
- [6] A.A. Kolender, C.A. Pujol, E.B. Damonte, M.C. Matulewicz, A.S. Cerezo, *Carbohydr. Res.*, 304 (1997) 53–60.
- [7] H.H. Haines, M.C. Matulewicz, A.S. Cerezo, *Hydrobiologia*, 204–205 (1990) 637–643.
- [8] M.C. Matulewicz, H.H. Haines, A.S. Cerezo, *Phytochemistry*, 36 (1994) 97–103.
- [9] M. Karas, D. Bachmann, U. Bahr, F. Hillenkamp, *Int. J. Mass Spectrom. Ion Process.*, 78 (1987) 53–68.
- [10] K. Tanaka, H. Waki, Y. Ido, S. Akita, Y. Yoshida, T. Yoshida, *Rapid Commun. Mass Spectrom.*, 2 (1988) 151–153.
- [11] R.C. Beavis, B.T. Chait, *Rapid Commun. Mass Spectrom.*, 3 (1989) 233–235.
- [12] J. Lemoine, F. Chirat, B. Domon, *J. Mass Spectrom.*, 31 (1996) 908–912.
- [13] A.O. Chizhov, A. Dell, H.R. Morris, A.J. Reason, S.M. Haslam, R.A. McDowell, O.S. Chizhov, A.I. Usov, *Carbohydr. Res.*, 310 (1998) 203–210.
- [14] B. Stahl, A. Linos, M. Karas, F. Hillenkamp, M. Steup, *Anal. Biochem.*, 246 (1997) 195–204.
- [15] B. Stahl, M. Steup, M. Karas, F. Hillenkamp, *Anal. Chem.*, 63 (1991) 1463–1466.
- [16] D.J. Harvey, P.M. Rudd, R.H. Bateman, R.S. Bordoli, K. Howes, J.B. Joyes, R.G. Vickers, *Org. Mass Spectrom.*, 29 (1994) 753–765.
- [17] P. Juhasz, K. Biemann, *Carbohydr. Res.*, 270 (1995) 131–147.
- [18] H. Nonami, S. Fukui, R. Erra-Balsells, *J. Mass Spectrom.*, 32 (1997) 287–296.
- [19] Y. Dai, R.M. Whittall, C.A. Bridges, Y. Isogai, O. Hindsgaul, L. Li, *Carbohydr. Res.*, 304 (1997) 1–9.

- [20] D.J. Harvey, *Rapid Commun. Mass Spectrom.*, 7 (1993) 614–619.
- [21] M.D. Mohr, K.O. Bornsen, H.M. Widmer, *Rapid Commun. Mass Spectrom.*, 9 (1995) 809–814.
- [22] J.T. Park, M.J. Johnson, *J. Biol. Chem.*, 181 (1949) 149–151.
- [23] H. Nonami, K. Tanaka, Y. Fukuyama, R. Erra-Balsells, *Rapid Commun. Mass Spectrom.*, 12 (1998) 285–296.